Loss of CDKL5 disrupts kinome profile and event-related potentials leading to autistic-like phenotypes in mice

I-Ting Judy Wang[a], Megan Allen[a], Darren Goffin[a], Xinjian Zhu[b,c], Andrew H. Fairless[d], Edward S. Brodkin[d], Steve J. Siegel[d], Eric D. Marsh[b,c], Julie A. Blendy[e], and Zhaolan Zhou[a,1]

Departments of [a]Genetics, [b]Neurology, [d]Psychiatry, and [e]Pharmacology, Perelman School of Medicine at the University of Pennsylvania, Philadelphia, PA 19104; and [c]Division of Child Neurology, Department of Pediatrics and Neurology, Children's Hospital of Philadelphia, Philadelphia, PA 19104

Mutations in the X-linked cyclin-dependent kinase-like 5 (CDKL5) gene have been identified in neurodevelopmental disorders including atypical Rett syndrome (RTT), autism spectrum disorders (ASDs), and early infantile epileptic encephalopathy. The biological function of CDKL5 and its role in the etiology of these disorders, however, remain unclear. Here we report the development of a unique knockout mouse model of CDKL5-related disorders and demonstrate that mice lacking CDKL5 show autistic-like deficits in social interaction, as well as impairments in motor control and fear memory. Neurophysiological recordings reveal alterations in event-related potentials (ERPs) similar to those observed in RTT and ASDs. Moreover, kinome profiling uncovers disruption of multiple signal transduction pathways, including the AKT-mammalian target of rapamycin (mTOR) cascade, upon Cdkl5 loss-of-function. These data demonstrate that CDKL5 regulates signal transduction pathways and mediates autistic-like phenotypes and together establish a causal role for Cdkl5 loss-of-function in neurodevelopmental disorders.

Cyclin-dependent kinase-like 5 (CDKL5) is an X-linked gene associated with early infantile epileptic encephalopathy 2 (EIEE2) (1), atypical Rett syndrome (RTT) (2), and autism spectrum disorders (ASDs) (3, 4). Patients with CDKL5 mutations display a heterogenous array of clinical phenotypes, the most prominent of which include early-onset seizures, intellectual disability, and autistic features (5).

CDKL5 is a serine/threonine (S/T) kinase that is highly expressed in the brain (6). In vitro studies have demonstrated that CDKL5 may mediate the phosphorylation of methyl-CpG binding protein 2 (MeCP2) (7), DNA methyltransferase 1 (DNMT1) (8), and netrin-G1 ligand (NGL-1) (9). RNAi-mediated knockdown studies show that CDKL5 can regulate neuronal outgrowth and synapse stability (9, 10). Despite these proposed functions, the exact role of CDKL5 in the phosphorylation of MeCP2 (7, 11) and in dendritic outgrowth (9, 10) remains unclear, and thus requires further investigation. The limited understanding of CDKL5 function and its associated signal transduction pathways has hindered the development of therapeutics for CDKL5-related disorders. Current treatments focus on managing symptoms and reducing seizure frequency, but have limited effectiveness (12).

To investigate the function of CDKL5 in a disease model and identify potential avenues of therapeutic intervention, we developed a Cdkl5 knockout mouse. We found that mice lacking CDKL5 show autistic-like behavioral abnormalities, deficits in neural circuit communication, and alterations in multiple signal transduction pathways. We establish a causal link between Cdkl5 loss-of-function and disease-related phenotypes and identify the AKT-mammalian target of rapamycin (mTOR) pathway as a unique candidate for targeted therapeutic intervention of CDKL5-related disorders.

Results

Generation of Cdkl5 Knockout Mice. To investigate the pathophysiology underlying CDKL5-related disorders, we generated a Cdkl5 knockout mouse that models a splice site mutation found in a CDKL5 patient. This mutation results in the skipping of human CDKL5 exon 7, generating a premature termination codon and causing an early truncation of CDKL5 in its N-terminal kinase domain, thereby disrupting kinase activity (13). To mimic the effects of this splice site mutation, we deleted mouse Cdkl5 exon 6 through homologous-mediated recombination in ES cells (Fig. 1A). Deletion of Cdkl5 exon 6 leads to a similar shift in the reading frame and premature truncation within the N-terminal kinase domain (Fig. 1 A and B). The absence of Cdkl5 exon 6 at the DNA and mRNA levels was verified by PCR of genomic DNA and sequencing of cDNA prepared from Cdkl5 knockout mouse brains (Fig. 1 C and D). Loss of full-length CDKL5 protein was verified by Western blot (Fig. 1E). A truncated CDKL5 protein product in neurons isolated from Cdkl5 knockout mice has not been detected by antibodies raised against CDKL5 N- or C-terminal domains, likely due to nonsense stop codon mediated mRNA decay (Fig. S1A). In addition, female heterozygotes show decreased CDKL5 protein expression relative to WT female mice, as expected from X-linked mosaicism (Fig. S1B). Thus, deletion of Cdkl5 exon 6 likely represents a loss-of-function mutation. Experimental mice have been backcrossed onto the C57BL/6 background for at least six generations. Male mice lacking CDKL5 (Cdkl5$^{-/y}$) and female heterozygotes (Cdkl5$^{-/+}$) are viable, fertile, and display normal appearance, growth, and overall brain morphology (Fig. S1 C and D).

Hyperactivity, Motor Impairments, and Decreased Anxiety in Cdkl5$^{-/y}$ Mice. Given the clinical relevance of CDKL5-related disorders in males (14, 15) and the confounding effects of mosaic CDKL5 expression in females from random X-chromosome inactivation, we characterized the behavioral profile of Cdkl5 knockouts in male (Cdkl5$^{-/y}$) mice, compared with wild-type male littermates (WT, Cdkl5$^{+/y}$). We found that Cdkl5$^{-/y}$ mice exhibit motor and anxiety impairments similar to those observed in other ASD and RTT mouse models (2, 16–19). In a locomotor assay within a home cage-like environment, Cdkl5$^{-/y}$ mice demonstrated significantly higher motor activity relative to WT littermate controls
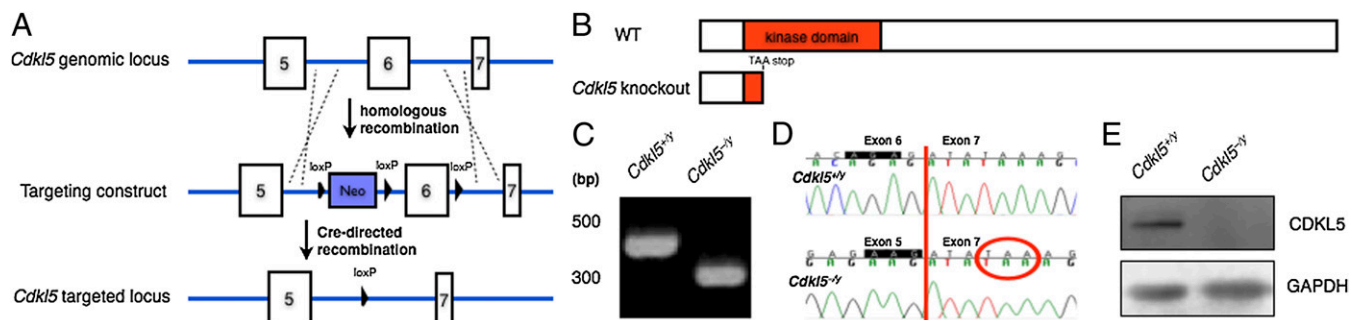
Fig. 1. Generation of *Cdkl5* knockout mice. (*A*) Targeting strategy. Three loxP sites and a neomycin positive selection cassette (Neo) were inserted surrounding the genomic locus of *Cdkl5* exon 6 via homologous recombination. Upon Cre-directed recombination, both the Neo cassette and exon 6 were excised. (*B*) Schematic of CDKL5 protein in WT and knockout. The excision of exon 6 causes a reading frame shift, resulting in a TAA stop codon in the 5′ end of exon 7, leading to truncation of CDKL5 in its kinase domain (red). (*C*) PCR of genomic DNA using primers flanking exon 6. A 300-bp PCR product in *Cdkl5*$^{-/y}$ mice indicates the absence of *Cdkl5* exon 6. (*D*) Sequencing of cDNA generated from *Cdkl5* mRNA. Excision of exon 6 in *Cdkl5*$^{-/y}$ mice causes the reading frame, highlighted in black, to be shifted in *Cdkl5*$^{-/y}$ mice, resulting in a premature stop codon (TAA, circled in red) at the 5′ end of exon 7. (*E*) Western blot probed with an antibody directed against CDKL5. Full-length CDKL5 protein is absent in *Cdkl5*$^{-/y}$ mice.

(Fig. 2*A*). Similar hyperactivity was also observed in the zero maze test and social approach test (Fig. S2 *A* and *B*).

On an accelerating rotarod assay, the latency to fall in *Cdkl5*$^{-/y}$ mice increased across trials similarly to that of WT mice, but was consistently lower than that of WT (Fig. 2*B*), indicating that *Cdkl5*$^{-/y}$ mice have comparable motor learning but impaired motor coordination relative to their WT littermates. *Cdkl5*$^{-/y}$ mice also showed decreased anxiety-related behavior in a zero maze test similar to that of *Mecp2* mouse models of RTT, spending more time in open areas and less time in the closed areas relative to WT littermates (Fig. 2*C*). In addition, we have observed hindlimb and forelimb clasping in *Cdkl5*$^{-/y}$ mice (Fig. S2*C*), a phenotype also exhibited in *Mecp2* mouse models (19–22). These data demonstrate that *Cdkl5*$^{-/y}$ mice exhibit hyperactivity, impaired motor control, and decreased anxiety, phenotypes that have also been observed in ASD and RTT patients (2, 5, 23).

Autistic-Like Social Behavior in *Cdkl5*$^{-/y}$ Mice. Given that deficits in social interaction are a hallmark feature of ASDs and are prevalent in patients with *CDKL5* mutations (5, 24), we next examined sociability using a three-chambered social approach test and found that mice lacking CDKL5 demonstrate profound impairment in social interaction. During the initial habituation phase, both WT and *Cdkl5*$^{-/y}$ mice explored both chambers equally, demonstrating no initial chamber preference (Fig. S2*D*). However, upon introduction of a novel object into one chamber (nonsocial chamber, NS) and a novel gonadectomized male A/J stimulus mouse into the other chamber (social chamber, S), *Cdkl5*$^{-/y}$ mice showed reduced social preference relative to WT mice, spending less time in the social chamber and more time in the nonsocial chamber relative to WT mice (Fig. 2*D*). In addition, *Cdkl5*$^{-/y}$ mice spent more time sniffing the novel object and a trend toward less time sniffing the novel stimulus mouse relative to WT mice (Fig. 2*E*). Furthermore, when barriers were

Fig. 2. Behavioral phenotyping of *Cdkl5*$^{-/y}$ mice. (*A*) Sixty-minute locomotor assay, measured by infrared beam breaks in a home cage-like environment. *Cdkl5*$^{-/y}$ mice (*n* = 19) display increased activity relative to wild type (WT, *Cdkl5*$^{+/y}$) littermates (*n* = 15). Two-way repeated measures (RM) ANOVA, *P* < 0.0001 (interaction). (*B*) Rotarod assay, measuring latency to fall from an accelerating rotating rod. Testing was performed five trials per day for 5 consecutive days. Latency to fall is decreased in *Cdkl5*$^{-/y}$ mice (*n* = 18) relative to WT littermates (*n* = 15), indicating impaired motor coordination in *Cdkl5*$^{-/y}$ mice. Two-way ANOVA, *P* < 0.01 (main effect of genotype). (*C*) *Cdkl5*$^{-/y}$ mice (*n* = 14) spend more time in the open arms and less time in the closed arms of a zeromaze assay relative to WT littermates (*n* = 12), showing decreased anxiety. **P* < 0.05, unpaired two-tailed Student *t* test. (*D*) Three-chambered social approach assay. *Cdkl5*$^{-/y}$ mice (*n* = 17) spend less time in a social chamber containing a stimulus mouse (S) and more time in a nonsocial chamber containing a novel object (NS) relative to WT mice (*n* = 15). C, center. Two-way ANOVA with Bonferroni correction, *P* < 0.0001 (interaction); ***P* < 0.01, ****P* < 0.001. (*E*) *Cdkl5*$^{-/y}$ mice (*n* = 17) spend significantly more time sniffing a novel object (NS) and trend toward less time sniffing a stimulus mouse (S) relative to WT mice (*n* = 15). Two-way ANOVA with Bonferroni correction, *P* < 0.01 (interaction); **P* < 0.05. (*F*) *Cdkl5*$^{-/y}$ mice (*n* = 17) spend less time directly interacting with a freely moving stimulus mouse compared with WT littermates (*n* = 15). ****P* < 0.001, unpaired two-tailed Student *t* test. (*G*) *Cdkl5*$^{-/y}$ mice (*n* = 12) show impaired nesting behavior relative to WT littermates (*n* = 11) at 4–5 postnatal weeks. ****P* < 0.001, unpaired two-tailed Student *t* test. (*H*) Fear conditioning paradigm, measuring time spent immobile. While *Cdkl5*$^{-/y}$ mice (*n* = 14) freeze in response to a mild footshock similarly to WT littermates (postshock), they show decreased freezing upon return to the testing chamber (context) and upon hearing the testing tone (cue) relative to WT littermates (*n* = 14), demonstrating impaired learning and memory in *Cdkl5*$^{-/y}$ mice. Two-way ANOVA with Bonferroni correction, *P* < 0.01 (interaction); **P* < 0.05. All data are presented as mean ± SEM.

Wang et al.
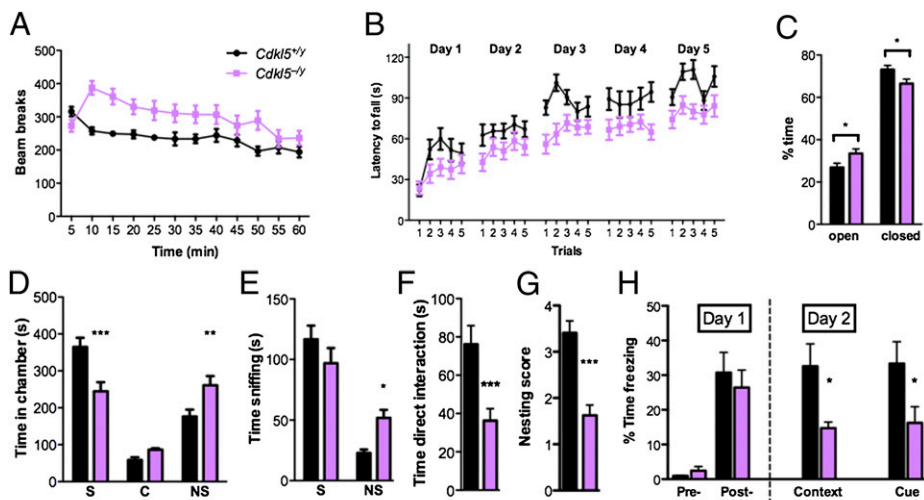
removed to allow freely mobile direct interaction, *Cdkl5*$^{-/y}$ mice spent significantly less time interacting (sniffing, allogrooming) with the stimulus mouse compared with WT littermates (Fig. 2*F*).

Cdkl5$^{-/y}$ mice also displayed impaired nesting, a phenotype related to home-cage social behavior that has been observed in ASD and RTT mouse models (17, 25, 26) (Fig. 2*G*). Importantly, we found no olfaction impairments in either genotype (Fig. S2*E*), suggesting that the social deficits in *Cdkl5*$^{-/y}$ mice are not the secondary consequence of an inability to discriminate between social and neutral odors. Together, these data demonstrate that *Cdkl5*$^{-/y}$ mice have ASD-like deficits in social behavior.

Impaired Learning and Memory in *Cdkl5*$^{-/y}$ Mice. Because intellectual disability is a common clinical phenotype among CDKL5 patients (12), we also assessed learning and memory in *Cdkl5* knockout mice using context- and cue-dependent fear conditioning. During the acquisition phase, both WT and *Cdkl5*$^{-/y}$ mice showed similar exploratory behavior before the foot shock and similar freezing behavior immediately following the foot shock (Fig. 2*H*). When reexposed to the shock box or paired tone 24 h later, *Cdkl5*$^{-/y}$ mice froze significantly less than WT littermates, indicating impaired contextual and cued fear memory (Fig. 2*H*). Taken together, these behavioral studies demonstrate that mice lacking CDKL5 have deficits in motor function, social behavior, and learning and memory.

Normal EEG Patterns and Absence of Spontaneous Seizures in *Cdkl5*$^{-/y}$ Mice. Given the prevalence of intractable seizures in patients with *CDKL5* mutations (12), we next examined the occurrence of spontaneous seizures in *Cdkl5* knockout mice through video-EEG recordings. We did not, however, observe any spontaneous seizures in *Cdkl5*$^{-/y}$ mice recorded for at least 72 h, with some mice recorded for as long as 240 h. Consistent with this finding, the basal EEG patterns and power distribution across different oscillation frequencies in *Cdkl5*$^{-/y}$ mice were similar to that of WT littermates (Fig. S3 *A* and *B*). Despite the large degree of homology between the murine and human CDKL5 protein, the absence of spontaneous seizures observed in our *Cdkl5*$^{-/y}$ mice may reflect a distinct function or modification of CDKL5 in humans that is absent in lower organisms. Moreover, the C57BL/6 genetic background is known to confer increased seizure resistance (27), thus potentially occluding spontaneous seizures in our *Cdkl5*$^{-/y}$ mice.

Event-Related Potential Deficits in *Cdkl5*$^{-/y}$ Mice. The absence of spontaneous seizures in *Cdkl5*$^{-/y}$ mice, however, allowed us to examine neural circuit deficits that are mediated by *Cdkl5* loss-of-function rather than the secondary consequence of seizures. Sensory information processing measured as an event-related potential (ERP) has recently been proposed as a biomarker to monitor neural circuit function in ASD and RTT animal models (19, 28, 29). We therefore recorded auditory-evoked ERPs in adult WT and *Cdkl5*$^{-/y}$ mice, as these ERP assessments can be performed on nonanesthetized, freely mobile mice and are not confounded by the motor and cognitive deficits observed in *Cdkl5*$^{-/y}$ mice. Compared with the characteristic amplitude and latency of the P1 (positive), N1 (negative), and P2 polarity peaks in WT mice, *Cdkl5*$^{-/y}$ mice display an aberrant ERP waveform (Fig. 3*A*). We observed a significant decrease in the amplitude of the N1 and P2 peaks and a significant increase in latency of the P2 peak (Fig. 3 *A–C*). Importantly, auditory brainstem recordings detected no hearing impairments in either genotype. As the amplitude and latency of these polarity peaks are believed to reflect the strength and timing of cognitive processes, these data indicate that *Cdkl5* loss-of-function disrupts neural circuit communication. Notably, patients with ASD and RTT have alterations in both amplitude and latencies of ERPs (30, 31).

Disruption of Low-Frequency Event-Related Neuronal Oscillations in *Cdkl5*$^{-/y}$ Mice. Circuit communication is composed of neuronal oscillations over a range of frequencies. We therefore also performed time–frequency analysis of the ERPs to examine frequency-specific changes in instantaneous power and phase locking in response to the auditory stimuli. *Cdkl5*$^{-/y}$ mice demonstrated reduced oscillatory strength specifically at low frequencies, showing attenuated event-related depression in the low-frequency delta (δ, 2–4 Hz), theta (θ, 4–8 Hz), and alpha (α, 8–12 Hz) oscillations, but no difference in the high-frequency beta (β, 12–30 Hz), low gamma (γ_{low}, 30–50 Hz), and high gamma (γ_{high}, 70–140 Hz) oscillations relative to WT controls (Fig. 3 *D* and *E* and Fig. S4*A*). Similarly, event-related phase locking, which reflects the reliability and sensitivity of circuit communication, and is measured by the phase-locking factor (PLF), were also significantly decreased in *Cdkl5*$^{-/y}$ mice exclusively in the low-frequency δ, θ, and α oscillations relative to WT littermates (Fig. 3 *F* and *G* and Fig. S4*B*). Given that oscillatory activity in low-frequency ranges is associated with long-range neuronal circuit communication and high-frequency oscillations with local circuit communication (28, 32), our data suggest that ERP deficits in *Cdkl5*$^{-/y}$ mice may be mediated by impairments in long-range communication. Notably, EEG studies in ASD children have reported specific deficits in low-frequency δ, θ, and α oscillations (33, 34), indicating that similar neuronal network defects exist in *Cdkl5*$^{-/y}$ mice and ASD patients.

Disrupted Kinome Profile in *Cdkl5*$^{-/y}$ Mice. Given the highly conserved S/T kinase domain in CDKL5 (Fig. 1*B*), we reasoned that *Cdkl5* loss-of-function may disrupt phosphorylation of CDKL5 kinase substrates and related signaling pathways, thereby mediating deficits in neuronal network communication and autistic-like behaviors in *Cdkl5*$^{-/y}$ mice. Previous studies have reported that CDKL5 may mediate the phosphorylation of MeCP2 (7), DNMT1 (8), and NGL-1 (9) in vitro. The CDKL5 substrates in vivo, however, remain unknown. Therefore, to investigate the signaling networks affected by the absence of CDKL5 in vivo in an unbiased manner, we surveyed the S/T kinome profile in *Cdkl5* knockout mice, assessing the consequence of *Cdkl5* loss-of-function on overall S/T phosphorylation events. Because CDKL5 expression is enriched in the forebrain regions of the striatum, cortex, and hippocampus (Fig. S5), we probed brain-region–specific lysate from WT and *Cdkl5*$^{-/y}$ mice with multiple antibodies developed against a large set of well-characterized S/T phosphorylation motifs (35, 36). We identified a range of phosphorylation profiles affected by the loss of CDKL5 (Fig. 4*A*). Of these, the phosphorylation of adenosine monophosphate-activated protein kinase (AMPK), protein kinase A (PKA), and AKT substrates were strongly decreased in *Cdkl5*$^{-/y}$ mice (Fig. 4 *B* and *C* and Fig. S6), whereas other phosphorylation profiles were moderately or mildly affected [e.g., mitogen-activated protein kinase (MAPK), ataxia-telangiectasia mutated/ataxia-telangiectasia and Rad3-related (ATM/ATR), and cyclin-dependent kinase (CDK) substrates] (Fig. 4*A* and Figs. S7 and S8). Importantly, changes in phosphorylation profiles were clearly evident in forebrain regions including the striatum, somatosensory cortex, and hippocampus where CDKL5 is enriched and less pronounced in hindbrain regions including the brainstem where CDKL5 expression is low (Fig. 4 *B* and *C* and Figs. S5–S7), supporting a role of CDKL5 in the regulation of these pathways.

Disruption of AKT–mTOR Signaling in *Cdkl5*$^{-/y}$ Mice. The changes in the AMPK, AKT, PKC, and MAPK phosphorylation profiles suggested a convergence on the downstream signaling of phosphatase and tensin homolog (PTEN). Notably, mutations and dysfunction of components of this pathway, including PTEN, AKT, tuberous sclerosis complex (TSC), and mTOR, have been
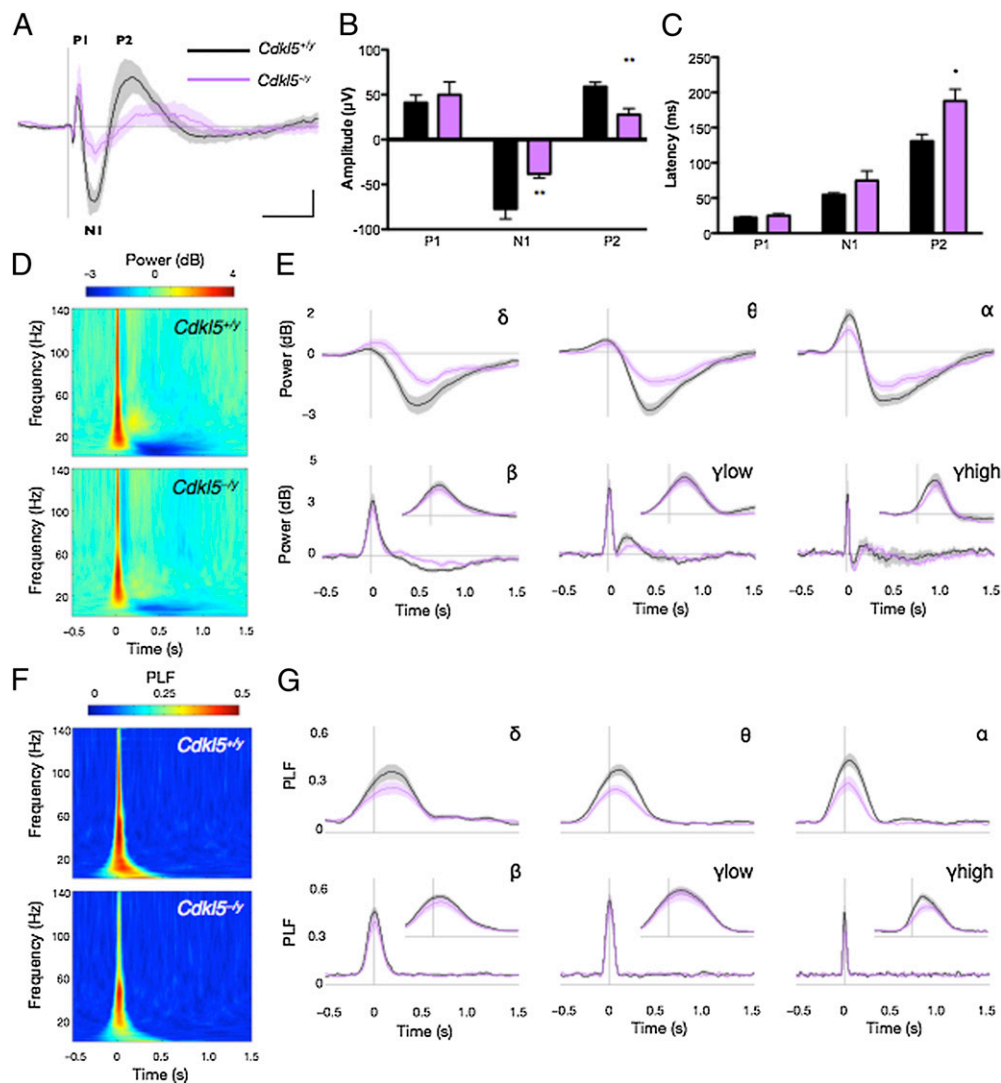
Fig. 3. *Cdkl5⁻/ʸ* mice display impaired ERP waveform and decreased event-related power and phase locking. (*A*) Grand-average ERP waveform following presentation of 250 85-dB white noise stimuli with 4-s interstimulus intervals in adult WT (*Cdkl5⁺/ʸ*) (*n* = 9) and *Cdkl5⁻/ʸ* mice (*n* = 9). Traces represent mean amplitude ± SEM. Characteristic polarity peaks P1, N1, and P2 in WT are labeled. [Scale bar, 100 ms (horizontal) and 20 mV (vertical).] (*B*) Amplitude and (*C*) latency of ERP peaks. Bars represent mean ± SEM; **P < 0.01, *P < 0.05, unpaired two-tailed Student *t* test with Bonferroni correction. (*D*) Time–frequency plots showing changes in event-related power following an 85-dB auditory stimulus. Color represents mean power, where warmer colors correspond to increased power and cooler colors correspond to decreased power relative to prestimulus baseline. (*E*) Changes in event-related mean power averaged across δ (2–4 Hz), θ (4–8 Hz), α (8–12 Hz), β (12–30 Hz), γ_low (30–50 Hz), and γ_high (70–140 Hz) oscillation frequencies. (Scale bars, length of a single δ oscillation cycle.) *Insets* show power traces on an expanded timescale, denoted by the length of a single oscillation cycle. Traces represent mean amplitude ± SEM. (*F*) Time–frequency plots showing changes in event-related phase-locking factor (PLF) following an 85-dB auditory stimulus. Color represents PLF, where warmer colors correspond to a higher PLF or lower circular variance in EEG phase across trials. (*G*) Changes in event-related PLF averaged across frequencies described above. (Scale bars, length of a single oscillation cycle.) *Insets* show traces on an expanded timescale. Traces represent mean PLF ± SEM.

linked to ASDs, RTT, and epileptic encephalopathies (18, 37, 38). To validate the disruption of AKT–mTOR signaling in *Cdkl5⁻/ʸ* mice, we measured the phosphorylation of AKT S473 and mTOR S2448 and found decreased phosphorylation of both AKT and mTOR in *Cdkl5⁻/ʸ* mice, with no concomitant alteration in total AKT or mTOR protein levels (Fig. 4 *D–H*). As phosphorylation of these residues promote AKT activation and mTOR complex 1 (mTORC1) assembly, respectively (39, 40), this finding is consistent with the overall decreased phosphorylation of AKT substrates in *Cdkl5⁻/ʸ* mice (Fig. 4*C* and Fig. S6 *B and D*) and likely reflect decreased AKT and mTORC1 activity upon *Cdkl5* loss-of-function. Together, we conclude that multiple signal transduction pathways, including the AKT–mTOR cascade, are disrupted upon the absence of CDKL5.

Discussion

In this study, we show that loss of CDKL5 in mice results in autistic-like behavioral deficits, impairment in neuronal communication, and disruptions in serine/threonine phosphorylation profiles. We establish a unique causal relationship between *Cdkl5* loss-of-function and disease-related phenotypes.

Core characteristics of CDKL5-related disorders include early-onset seizures, severe intellectual disability, and autistic-like features. In our behavioral analysis, we found that our *Cdkl5* knockout mice mirror the latter features, but not early-onset seizures. *Cdkl5⁻/ʸ* mice display hyperactivity, motor defects, reduced anxiety, decreased sociability, and impaired learning and memory. These phenotypes have been described in other ASD and RTT mouse models (2, 16, 17, 19, 26) and may mimic the
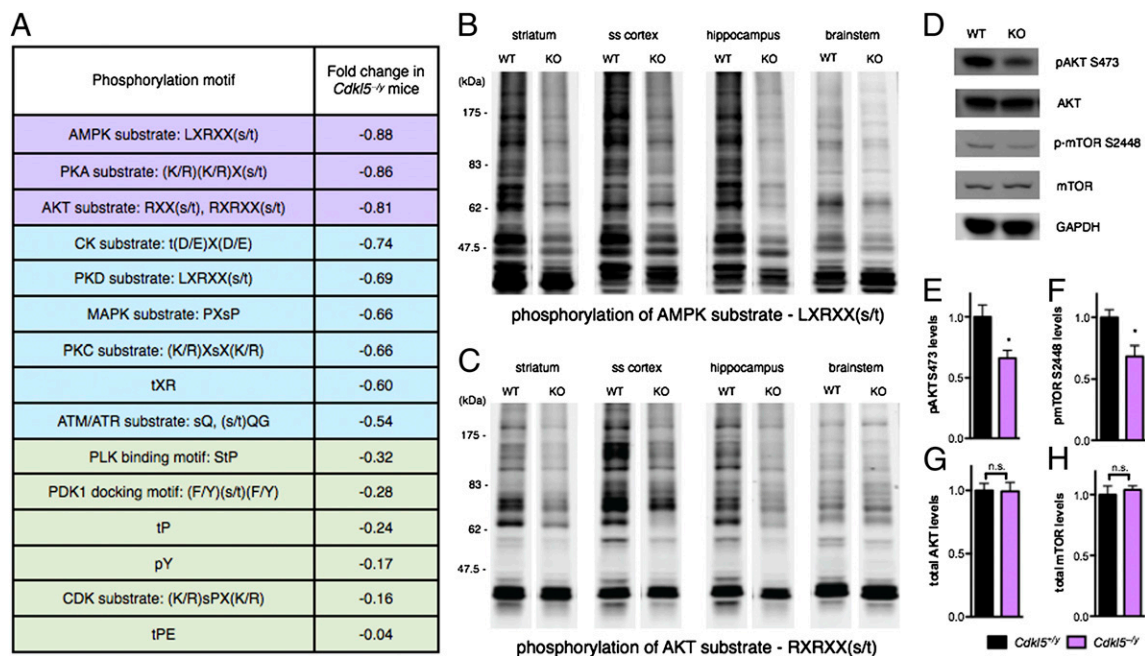
Wang et al.

www.manaraa.com

NEUROSCIENCE

Fig. 4. Altered kinome profile and disrupted AKT–mTOR signaling in *Cdkl5*$^{-/y}$ mice. (*A*) Summary of changes in kinome profile in *Cdkl5*$^{-/y}$ mice relative to WT littermates. Whole cell lysates from the cerebellum, striatum, somatosensory cortex, olfactory bulb, hippocampus, and brainstem of WT (*n* = 7) and *Cdkl5*$^{-/y}$ mice (*n* = 8) were probed with antibodies raised against different phosphorylation motifs representing known S/T kinases. Western blots were quantified using the Odyssey Infrared Imaging system and fold change in phosphorylation level between *Cdkl5*$^{-/y}$ and WT mice across the six brain regions are expressed as log$_2$ (phosphorylation level in WT over phosphorylation level in *Cdkl5*$^{-/y}$). Color scheme indicates relative degree of phosphorylation reduction in *Cdkl5*$^{-/y}$ mice: purple, strong; blue, moderate; and green, mild. (*B* and *C*) Whole cell lysate probed with an antibody specific for an RXRXX(s/t) phosphorylation motif representing AKT kinase substrates (*B*) and an antibody specific for an LXRXX(s/t) phosphorylation motif representing AMPK kinase substrates (*C*) shows a marked decrease in phosphorylation profiles in *Cdkl5*$^{-/y}$ mice (KO) relative to WT littermates in the striatum, somatosensory cortex (ss cortex), and hippocampus, but moderate decrease in the brainstem, consistent with regions of high and low CDKL5 expression, respectively. (*D*) AKT S473 and mTOR S2448 phosphorylation is reduced in whole brain lysate from *Cdkl5*$^{-/y}$ mice (KO) related to WT mice, whereas total levels of AKT and mTOR are unchanged. (*E* and *F*) Quantification of reduced AKT S473 (*E*) and mTOR S2448 (*F*) phosphorylation in *Cdkl5*$^{-/y}$ mice. Phosphorylated protein levels are normalized to GAPDH loading control and expressed relative to WT levels. *$P < 0.05$, unpaired two-tailed Student *t* test with Bonferroni correction. (*G* and *H*) Quantification of total AKT (*G*) and mTOR (*H*) in WT and *Cdkl5*$^{-/y}$ mice. Protein levels are normalized to GAPDH loading control and expressed relative to WT levels. NS, not significant; unpaired two-tailed Student *t* test.

absence of hand skills, intellectual disability, hyperactivity, and poor response to social interactions that have been described in CDKL5 patients (12, 41).

While video-EEG monitoring revealed an absence of spontaneous seizures in *Cdkl5*$^{-/y}$ mice, ERP analysis showed attenuated and delayed ERP polarity peaks suggestive of impaired neuronal connectivity, which is consistent with findings in ASD and RTT patients (30, 31) and animal models (19, 28, 29). Importantly, these behavioral and electrophysiological impairments are unlikely the secondary effects of an epileptic neuronal network, suggesting they are consequences of *Cdkl5* loss-of-function.

Time–frequency analysis of ERPs identified a specific deficit in event-related δ, θ, and α low-frequency neuronal oscillations in *Cdkl5*$^{-/y}$ mice. Interestingly, abnormalities in low-frequency neuronal oscillations have been reported in ASD children (33, 34). In addition, impairments in α and γ oscillations have also been described in ASDs, as α is believed to function in attention suppression of distracting stimuli and γ in feature binding (42, 43). Alpha oscillations have also been proposed to mediate long-distance coordination of γ oscillations (44). Thus, our data suggest that the oscillatory network of *Cdkl5*$^{-/y}$ mice may resemble that of ASD, where γ oscillations themselves are not affected, but rather, their α-mediated long-distance coordination. Moreover, as θ oscillations are proposed to support encoding and retrieval of memory (45, 46), the impairment in event-related power and PLF at the θ frequency are consistent with the learning and memory deficits in *Cdkl5*$^{-/y}$ mice and the prominent intellectual disability observed in patients with CDKL5-related disorders.

Lastly, our S/T kinome study revealed that many signal transduction pathways are disrupted in *Cdkl5* knockout mice. Of these, many pathway components, including the AKT–mTOR pathway, have been implicated in the etiology of ASDs (18, 47). Given that mTOR is a known regulator of cell growth, proliferation, motility, and neural plasticity (48), one consequence of reduced AKT–mTOR activity in the absence of CDKL5 is the disruption of neuronal development. Accordingly, RNAi-mediated knockdown of CDKL5 results in impaired dendritic outgrowth, neuronal migration (10), and spine maturation (9). Together, these data suggest a mechanism by which CDKL5 regulates AKT–mTOR-mediated cellular development, thus implicating the AKT–mTOR pathway as a potential therapeutic target for treatment of patients with CDKL5-related disorders.

In addition to the AKT–mTOR pathway, we found that the phosphorylation profiles of kinases involved in synaptic plasticity, including PKA, PKC, and protein kinase D (PKD), as well as kinases involved in cellular metabolism, including AMPK, ATM/ATR, and casein kinase (CK) (Figs. S6 and S7) were also decreased in *Cdkl5*$^{-/y}$ mice. Although many of these signaling changes may be indirect effects of *Cdkl5* loss-of-function, these data suggest that CDKL5 plays a critical role in coordinating multiple signaling cascades. Indeed, CDKL5 has been shown to regulate brain-derived neurotropic factor (BDNF)-induced activation of Rho family small GTPase Rac1 (10) and deficits in synaptic plasticity are commonly described in ASDs (17, 49). Consistent with these cellular functions, we found that CDKL5 is predominantly localized in the cytoplasm (Fig. S9). Notably, links

Wang et al.

www.manaraa.com

between these signaling pathways have been previously described, as CK regulates glutamatergic synaptic transmission (50), ATM mediates AKT S473 phosphorylation (51), and mutations in ATM cause the neurodegenerative movement disorder ataxis telegiectasia (52). It is possible, therefore, that CDKL5 may serve to mediate cross-talk between these signaling pathways.

Our data support an increasing awareness that CDKL5-related disorders are an independent clinical entity with an independent pathogenic mechanism, rather than a subclass of RTT. Strikingly, only less than one-quarter of individuals with *CDKL5* mutations meet the criteria for the early-onset seizure variant of RTT (53, 54). Its genetic link to neurodevelopmental disorders and recent identification as an ASD hotspot for balanced chromosomal rearrangements (4) highlight the need to characterize CDKL5 biological function, understand the mechanisms underlying CDKL5-related disorders, and identify effective therapies targeted toward slowing or reversing disease progression. Our study, therefore, provides a framework and an animal model for mechanistic and therapeutic studies of CDKL5-related disorders.

Materials and Methods

All behavioral, EEG, ERP, and kinome studies were performed on adult mice 9–12 wk of age backcrossed onto a C57BL/6 background for at least six generations, unless otherwise indicated. For ERP studies, tripolar electrodes were implanted and ERP traces were obtained by averaging single trial epochs of 250 white-noise stimuli of 10-ms duration, 85-dB sound pressure, and 4-s interstimulus intervals.

Data are reported as mean ± SEM, and statistical analysis was performed using GraphPad Prism software.

Other materials and methods are presented in *SI Materials and Methods*.

1. Nabbout R, Dulac O (2011) Epilepsy. Genetics of early-onset epilepsy with encephalopathy. *Nat Rev Neurol* 8(3):129–130.
2. Chahrour M, Zoghbi HY (2007) The story of Rett syndrome: From clinic to neurobiology. *Neuron* 56(3):422–437.
3. Sakai Y, et al. (2011) Protein interactome reveals converging molecular pathways among autism disorders. *Sci Transl Med* 3(86):86ra49.
4. Talkowski ME, et al. (2012) Sequencing chromosomal abnormalities reveals neurodevelopmental loci that confer risk across diagnostic boundaries. *Cell* 149(3):525–537.
5. Bahi-Buisson N, et al. (2008) Key clinical features to identify girls with CDKL5 mutations. *Brain* 131(Pt 10):2647–2661.
6. Kilstrup-Nielsen C, et al. (2012) What we know and would like to know about CDKL5 and its involvement in epileptic encephalopathy. *Neural Plast* 2012:728267.
7. Mari F, et al. (2005) CDKL5 belongs to the same molecular pathway of MeCP2 and it is responsible for the early-onset seizure variant of Rett syndrome. *Hum Mol Genet* 14(14):1935–1946.
8. Kameshita I, et al. (2008) Cyclin-dependent kinase-like 5 binds and phosphorylates DNA methyltransferase 1. *Biochem Biophys Res Commun* 377(4):1162–1167.
9. Ricciardi S, et al. (2012) CDKL5 ensures excitatory synapse stability by reinforcing NGL-1-PSD95 interaction in the postsynaptic compartment and is impaired in patient iPSC-derived neurons. *Nat Cell Biol* 14(9):911–923.
10. Chen Q, et al. (2010) CDKL5, a protein associated with Rett syndrome, regulates neuronal morphogenesis via Rac1 signaling. *J Neurosci* 30(38):12777–12786.
11. Lin C, Franco B, Rosner MR (2005) CDKL5/Stk9 kinase inactivation is associated with neuronal developmental disorders. *Hum Mol Genet* 14(24):3775–3786.
12. Bahi-Buisson N, Bienvenu T (2012) CDKL5-related disorders: From clinical description to molecular genetics. *Mol Syndromol* 2(3-5):137–152.
13. Archer HL, et al. (2006) CDKL5 mutations cause infantile spasms, early onset seizures, and severe mental retardation in female patients. *J Med Genet* 43(9):729–734.
14. Liang J-S, et al. (2011) CDKL5 alterations lead to early epileptic encephalopathy in both genders. *Epilepsia* 52(10):1835–1842.
15. Moseley BD, Dhamija R, Wirrell EC, Nickels KC (2012) Historic, clinical, and prognostic features of epileptic encephalopathies caused by CDKL5 mutations. *Pediatr Neurol* 46(2):101–105.
16. Schmeisser MJ, et al. (2012) Autistic-like behaviours and hyperactivity in mice lacking ProSAP1/Shank2. *Nature* 486(7402):256–260.
17. Won H, et al. (2012) Autistic-like social behaviour in Shank2-mutant mice improved by restoring NMDA receptor function. *Nature* 486(7402):261–265.
18. Tsai PT, et al. (2012) Autistic-like behaviour and cerebellar dysfunction in Purkinje cell Tsc1 mutant mice. *Nature* 488(7413):647–651.
19. Goffin D, et al. (2012) Rett syndrome mutation MeCP2 T158A disrupts DNA binding, protein stability and ERP responses. *Nat Neurosci* 15(2):274–283.
20. Guy J, Hendrich B, Holmes M, Martin JE, Bird A (2001) A mouse Mecp2-null mutation causes neurological symptoms that mimic Rett syndrome. *Nat Genet* 27(3):322–326.
21. Shahbazian M, et al. (2002) Mice with truncated MeCP2 recapitulate many Rett syndrome features and display hyperacetylation of histone H3. *Neuron* 35(2):243–254.
22. Chao H-T, et al. (2010) Dysfunction in GABA signalling mediates autism-like stereotypies and Rett syndrome phenotypes. *Nature* 468(7321):263–269.
23. Geschwind DH (2009) Advances in autism. *Annu Rev Med* 60:367–380.
24. Abrahams BS, Geschwind DH (2008) Advances in autism genetics: On the threshold of a new neurobiology. *Nat Rev Genet* 9(5):341–355.
25. Samaco RC, et al. (2008) A partial loss of function allele of methyl-CpG-binding protein 2 predicts a human neurodevelopmental syndrome. *Hum Mol Genet* 17(12):1718–1727.
26. Peñagarikano O, et al. (2011) Absence of CNTNAP2 leads to epilepsy, neuronal migration abnormalities, and core autism-related deficits. *Cell* 147(1):235–246.
27. McLin JP, Steward O (2006) Comparison of seizure phenotype and neurodegeneration induced by systemic kainic acid in inbred, outbred, and hybrid mouse strains. *Eur J Neurosci* 24(8):2191–2202.
28. Gandal MJ, et al. (2010) Validating γ oscillations and delayed auditory responses as translational biomarkers of autism. *Biol Psychiatry* 68(12):1100–1106.
29. Liao W, Gandal MJ, Ehrlichman RS, Siegel SJ, Carlson GC (2012) MeCP2+/- mouse model of RTT reproduces auditory phenotypes associated with Rett syndrome and replicate select EEG endophenotypes of autism spectrum disorder. *Neurobiol Dis* 46(1):88–92.
30. Stauder JEA, Smeets EEJ, van Mil SGM, Curfs LGM (2006) The development of visual- and auditory processing in Rett syndrome: An ERP study. *Brain Dev* 28(8):487–494.
31. Roberts TPL, et al. (2010) MEG detection of delayed auditory evoked responses in autism spectrum disorders: Towards an imaging biomarker for autism. *Autism Res* 3(1):8–18.
32. Winterer G, et al. (2000) Schizophrenia: Reduced signal-to-noise ratio and impaired phase-locking during information processing. *Clin Neurophysiol* 111(5):837–849.
33. Dawson G, Klinger LG, Panagiotides H, Lewy A, Castelloe P (1995) Subgroups of autistic children based on social behavior display distinct patterns of brain activity. *J Abnorm Child Psychol* 23(5):569–583.
34. Stroganova TA, et al. (2007) Abnormal EEG lateralization in boys with autism. *Clin Neurophysiol* 118(8):1842–1854.
35. Zhang H, et al. (2002) Phosphoprotein analysis using antibodies broadly reactive against phosphorylated motifs. *J Biol Chem* 277(42):39379–39387.
36. Moritz A, et al. (2010) Akt-RSK-S6 kinase signaling networks activated by oncogenic receptor tyrosine kinases. *Sci Signal* 3(136):ra64.
37. Ricciardi S, et al. (2011) Reduced AKT/mTOR signaling and protein synthesis dysregulation in a Rett syndrome animal model. *Hum Mol Genet* 20(6):1182–1196.
38. Zhou J, Parada LF (2012) PTEN signaling in autism spectrum disorders. *Curr Opin Neurobiol* 22:873–879.
39. Bhaskar PT, Hay N (2007) The two TORCs and Akt. *Dev Cell* 12(4):487–502.
40. Rosner M, Siegel N, Valli A, Fuchs C, Hengstschläger M (2010) mTOR phosphorylated at S2448 binds to raptor and rictor. *Amino Acids* 38(1):223–228.
41. Willemsen MH, Rensen JHM, van Schrojenstein-Lantman de Valk HMJ, Hamel BCJ, Kleefstra T (2012) Adult phenotypes in Angelman- and Rett-Like syndromes. *Mol Syndromol* 2(3-5):217–234.
42. Foxe JJ, Snyder AC (2011) The role of alpha-band brain oscillations as a sensory suppression mechanism during selective attention. *Front Psychol* 2:154.
43. Uhlhaas PJ, Pipa G, Neuenschwander S, Wibral M, Singer W (2011) A new look at gamma? High- (>60 Hz) γ-band activity in cortical networks: Function, mechanisms and impairment. *Prog Biophys Mol Biol* 105(1-2):14–28.
44. Palva S, Palva JM (2007) New vistas for alpha-frequency band oscillations. *Trends Neurosci* 30(4):150–158.
45. Ward LM (2003) Synchronous neural oscillations and cognitive processes. *Trends Cogn Sci* 7(12):553–559.
46. Buzsáki G (2005) Theta rhythm of navigation: Link between path integration and landmark navigation, episodic and semantic memory. *Hippocampus* 15(7):827–840.
47. Jeste SS, Sahin M, Bolton P, Ploubidis GB, Humphrey A (2008) Characterization of autism in young children with tuberous sclerosis complex. *J Child Neurol* 23(5):520–525.
48. Zoncu R, Efeyan A, Sabatini DM (2011) mTOR: from growth signal integration to cancer, diabetes and ageing. *Nat Rev Mol Cell Biol* 12(1):21–35.
49. Peça J, et al. (2011) Shank3 mutant mice display autistic-like behaviours and striatal dysfunction. *Nature* 472(7344):437–442.
50. Chergui K, Svenningsson P, Greengard P (2005) Physiological role for casein kinase 1 in glutamatergic synaptic transmission. *J Neurosci* 25(28):6601–6609.
51. Viniegra JG, et al. (2005) Full activation of PKB/Akt in response to insulin or ionizing radiation is mediated through ATM. *J Biol Chem* 280(6):4029–4036.
52. Barlow C, et al. (1996) Atm-deficient mice: A paradigm of ataxia telangiectasia. *Cell* 86(1):159–171.
53. Fehr S, et al. (2012) The CDKL5 disorder is an independent clinical entity associated with early-onset encephalopathy. *Eur J Hum Genet*, 10.1038/ejhg.2012.156.
54. Neul JL, et al.; RettSearch Consortium (2010) Rett syndrome: Revised diagnostic criteria and nomenclature. *Ann Neurol* 68(6):944–950.

NEUROSCIENCE

Wang et al.

www.manaraa.com